

Mitochondrial Ribosomal RNA (rRNA) Methyltransferase Family Members Are Positioned to Modify Nascent rRNA in Foci near the Mitochondrial DNA Nucleoid*

Received for publication, September 3, 2013. Published, JBC Papers in Press, September 13, 2013, DOI 10.1074/jbc.M113.515692

Ken-Wing Lee, Cynthia Okot-Kotber¹, Joseph F. LaComb, and Daniel F. Bogenhagen²

From the Department of Pharmacological Sciences, Stony Brook University, Stony Brook, New York 11794-8651

Background: Mitochondrial rRNAs contain site-specific modifications, including methylated residues, but few of the enzymes responsible for these modifications have been found.

Results: RNMTL1, MRM1, and MRM2 are methyltransferase family members found associated with the mtDNA nucleoid and with the large ribosomal subunit.

Conclusion: The association of putative RNA-modifying enzymes with nucleoids and ribosomes supports the model that assembly of mitochondrial ribosomes begins while rRNA transcription continues.

Significance: This work advances understanding of the assembly of mitochondrial ribosomes necessary for biosynthesis of the respiratory chain.

We have identified RNMTL1, MRM1, and MRM2 (FtsJ2) as members of the RNA methyltransferase family that may be responsible for the three known 2'-O-ribose modifications of the 16 S rRNA core of the large mitochondrial ribosome subunit. These proteins are confined to foci located in the vicinity of mtDNA nucleoids. They show distinct patterns of association with mtDNA nucleoids and/or mitochondrial ribosomes in cell fractionation studies. We focused on the role of the least studied protein in this set, RNMTL1, to show that this protein interacts with the large ribosomal subunit as well as with a series of non-ribosomal proteins that may be involved in coupling of the rate of rRNA transcription and ribosome assembly in mitochondria. siRNA-directed silencing of RNMTL1 resulted in a significant inhibition of translation on mitochondrial ribosomes. Our results are consistent with a role for RNMTL1 in methylation of G¹³⁷⁰ of human 16 S rRNA.

Mammalian cells have retained a mitochondrial genome (mitochondrial DNA; mtDNA)³ to encode 13 mRNAs for subunits of respiratory complexes that are translated on mitochondrial ribosomes using a minimal set of 22 tRNAs. The mitochondrial small and large ribosomal subunits contain 12 S and 16 S rRNAs encoded by mtDNA. These RNAs represent minimized versions of bacterial 16 S and 23 S rRNAs. In mitochondria, the rRNAs are assembled with ~80 nucleus-encoded ribosomal proteins into 28 S and 39 S subunits that are relatively enriched in protein as compared with bacterial or eukaryotic ribosomes (1, 2). Roughly half of the mammalian mitochondrial ribosomal proteins have recognizable bacterial homologs, whereas the others have evolved as distinct proteins, many of

which are poorly conserved in yeast (3). Nevertheless, mammalian mitochondria exhibit sensitivity to some inhibitors of bacterial protein synthesis, such as chloramphenicol and linezolid (4), an important new anti-staphylococcal antibiotic.

In all kingdoms of life, rRNAs receive multiple post-transcriptional modifications that are critically important for translation (5), and mammalian mitochondrial rRNAs are no exception. However, the number of post-transcriptional modifications observed for mammalian mitochondrial rRNAs is sharply diminished in comparison with bacterial and human cytoplasmic rRNAs, which contain 33 and over 200 modifications, respectively. Most of the modifications of mammalian rRNA are site-specific methylations first characterized by Dubin's laboratory using cultured BHK-21 hamster cells (6, 7) (reviewed in Ref. 8). The small rRNA contains five sites of base modification but no methylated ribose residues. Only the dimethylation of two adjacent adenosine residues near the 3'-end of the rRNA has been studied extensively. These modifications of human A⁹³⁶ and A⁹³⁷ are introduced by TFB1M, a functional homolog of bacterial KsgA (9–11). The action of TFB1M has been shown to be essential for assembly of the small subunit and for embryonic development (12). Methylation of 12 S rRNA by TFB1M has recently been implicated in development of aminoglycoside-induced deafness (13). A second protein, ERAL1, has been shown to bind to a site overlapping the TFB1M methylation site, but its role in methylation or ribosome biogenesis is poorly understood (14, 15). The related prokaryotic Era protein is one of several GTPases that function in ribosome assembly (16).

The large rRNA contains three sites of methylation of 2'-O-ribose residues, a GmG residue at G¹¹⁴⁴ or G¹¹⁴⁵ and UmGm at U¹³⁶⁹G¹³⁷⁰ of the human 16 S rRNA. These sites are conserved in bacterial and cytoplasmic rRNAs, where they stabilize RNA structures critical for the peptidyltransferase reaction and tRNA recognition (5). These modifications have been studied in yeast rRNA, where methylation of the residue homologous to human G¹¹⁴⁵ has been attributed to MRM1/PET56 (17), and that analogous to U¹³⁶⁹ methylation is conducted by MRM2

* This work was supported in part by a Senior Scholar Award from the Ellison Medical Foundation (to D. F. B.).

¹ Recipient of an undergraduate National Institutes of Health MARC award.

² To whom correspondence should be addressed. E-mail: daniel.bogenhagen@stonybrook.edu.

³ The abbreviations used are: mtDNA, mitochondrial DNA; rRNA, ribosomal RNA; AdoMet, S-adenosylmethionine.

(18). Yeast rRNA evidently lacks the G¹³⁷⁰ methylation. Camara *et al.* (19) reported that deficiency of a complex of MTERF4 with the methyltransferase NSUN4 leads to ineffective assembly of the large ribosomal subunit. However, NSUN4 appears to be most closely related to m5C methyltransferases. Cytosine methylation has not been detected in 16 S rRNA, and the role for NSUN4 in the modification of backbone ribose residues is uncertain. Rorbach and Minczuk (8) have suggested that this complex may affect a site in 12 S rRNA required for interaction between the large and small subunits. However, in this regard, it is interesting to note that a yeast homolog of KsgA, Dim1p, can stimulate cytoplasmic ribosome biogenesis even when its active site has been inactivated (20), suggesting that simple binding of a methyltransferase can contribute to a checkpoint in ribosome assembly.

With the possible exception of NSUN4, the mammalian enzymes responsible for these 16 S rRNA modifications have not been identified. We recently identified a candidate mitochondrial methyltransferase, RNMTL1, in association with mtDNA nucleoids (21). The RNMTL1 primary structure features a 2'-O-ribose binding site and a SpoU methyltransferase domain, whereas the amino terminus of the mouse protein has a predicted 99% probability of serving as a mitochondrial import signal (Mitoprot; available on the Helmholtz Center Munich Web site). Thus, we considered that this protein may be involved in 16 S rRNA modification. Examination of the GenBankTM database and other resources revealed two additional putative methyltransferases, MRM1 and MRM2, containing N-terminal sequences with a 99 and 57% probability of mitochondrial import, respectively. Mouse RNMTL1, MRM1, and MRM2 were all identified in a broad proteomic analysis of mitochondria from mouse tissues (22), but none of these proteins have been studied individually as mitochondrial proteins. One report on human MRM2 referred to this protein as FTSJ2, one of at least three human genes related to the bacterial FtsJ methyltransferase (RLME) that conducts 2'-O-methylation of uridyl residues (23). In that report, fusion of GFP on the N terminus of MRM2/FTSJ2 resulted in a nucleolar location. Because this expression strategy would obscure an N-terminal mitochondrial localization signal, we reinvestigated this using a conventional C-terminal fluorescent protein reporter to document that it is, indeed, a mitochondrial protein.

In this paper, we report evidence that RNMTL1, MRM1, and MRM2 are all mtDNA nucleoid-associated mitochondrial proteins that probably participate in methylation of rRNA. We have focused on RNMTL1 in this report because it was this protein that we initially observed associated with nucleoids, and it has received no previous annotation as a mitochondrial protein. We found that this protein was associated with both nucleoids and ribosomes, establishing RNMTL1 as a subject for future detailed study of its role in ribosome assembly. We report that siRNA-directed depletion of RNMTL1 results in reduced efficiency of mitochondrial translation.

EXPERIMENTAL PROCEDURES

Materials—Oligonucleotides were obtained from Operon. Chemicals used are listed with their suppliers: tissue culture media, mifepristone, and zeocin (Invitrogen); hygromycin

B and Fugene 6 (Roche Applied Science); 60% iodixanol (Optiprep, Sigma-Aldrich); DNase I Type II (Sigma-Aldrich); TurboNuclease (Accelagen); AmplifyTM (Amersham Biosciences). Other reagents were from Sigma-Aldrich. Restriction endonucleases were from New England Biolabs. Triton X-100 was obtained as a 10% solution from Fisher. [γ -³²P]ATP and S-[³H]adenosylmethionine were obtained from MP Biochemicals. A mixture of [³⁵S]methionine/cysteine was obtained from PerkinElmer Life Sciences. His-Trap, heparin-Sepharose HiTrap, and Superose 6 chromatography columns were obtained from GE Healthcare.

Antibodies—Antibodies directed against specific antigens are listed with their suppliers and dilutions: SDHA (MitoSciences; 1:10,000), anti-FLAG (Sigma-Aldrich; 1:1,500), MRM1 (Sigma-Aldrich; 1:500), MRM2 (Abcam; 1:1000), MRPS15 (Proteintech; 1:1500), RNMTL1 (Proteintech; 1:5000), anti-DNA (Chemicon; 1:12,000), fluorescent goat-anti-rabbit or goat-anti-mouse secondary antibodies (Molecular Probes; 1:1000). Rabbit antibodies directed against human TFAM were generated in the Bogenhagen laboratory, and those directed against MRPL13 were a kind gift from Dr. Linda Spemulli (University of North Carolina; 1:1500 to 1:4000). Alkaline phosphatase-conjugated goat anti-mouse and goat anti-rabbit antibodies used for colorimetric detection were from KPL. In some cases, HRP-conjugated anti-rabbit or anti-mouse antibodies (Thermo Scientific) were used at a 1:5000 dilution for detection using chemiluminescence imaged using a CCD camera system (Alpha Imager) or x-ray film.

Cell Culture—Mouse 3T3 cells transfected with pSwitch (Hyg^R) to permit mifepristone induction were obtained from Invitrogen and are referred to as 3T3-Switch cells. These cells were transfected with a variety of pGS (Zeo^R) vectors containing cDNAs fused to the Eos fluorescent reporter (24) using Fugene 6, and stable cultures were obtained by selection on hygromycin B (50 μ g/ml) and zeocin (200 μ g/ml). For induction of genes encoded by the pGS vector, 50 pM mifepristone was applied for 16 h for biochemical isolation, or 100 pM mifepristone was added for 7 h for imaging. For fluorescent imaging of mitochondria, 50 nM MitoTracker Red was applied to live cells for at least 90 min prior to fixation. Suspension HeLa cells were cultured as described (21).

Cloning—Mouse RNMTL1, MRM1, and MRM2 were cloned from a first strand cDNA library (Clontech) with primers containing an *Asc*I restriction site on the 5'-side and a *Not*I restriction site on the 3'-side and was inserted into pGS-Eos (24), creating an in-frame fusion with the monomeric fluorescent protein Eos (25), generating pGS-mmRNMTL1-Eos, pGS-mmMRM1-Eos, and pGS-mmMRM2-Eos. The RNMTL1 insert was also transferred to pGS-FLAG₃-His₆ (pGS-3FH) vector constructed in the Bogenhagen lab containing the FLAG₃ and His₆ affinity tags in place of Eos. The predicted mature forms of human RNMTL1 and of mouse MRM1 and MRM2 lacking putative mitochondrial localization signals were cloned into the pET22b+ vector and expressed with a C-terminal His tag in *Escherichia coli* BL21 RIPL cells by induction with 1 mM isopropyl 1-thio- β -D-galactopyranoside at 37 °C for 3 h. Cells were lysed in a buffer containing 1 M KCl to dissociate protein-nucleic acid interactions, and the supernatant was successively purified on HisTrapTM (GE Healthcare)

RNA Methyltransferase Family Members at mtDNA Nucleoids

and Heparin HiTrapTM (GE Healthcare) columns following standard procedures. Human MTERF4-NSUN4 protein was kindly provided by the laboratory of Miguel Garcia-Diaz (Stony Brook University).

Immunofluorescence—3.5-cm diameter MatTek plates were coated with 15 $\mu\text{g}/\text{ml}$ fibronectin for 2 h to improve cell adhesion and blocked with DMEM supplemented with FBS for 20 min, and 50,000–80,000 cells were plated. Cells were fixed in 4% paraformaldehyde; permeabilized in PBS containing 0.25% Triton X-100; and blocked sequentially with MaxBlock (Active Motif) and 5% (v/v) horse serum, 3% (w/v) BSA, 0.2% Triton X-100 in PBS. Mouse anti-DNA antibodies were applied at a 1:12,000 dilution, rabbit anti-RNMTL1 antibodies were applied at 1:2000, and secondary antibodies were applied at 1:1000.

Cell Fractionation—All steps were conducted at 4 °C unless noted otherwise, and all buffers contained 0.2 mM PMSF, 5 $\mu\text{g}/\text{ml}$ leupeptin, and 1 μM pepstatin A. Purification of mitochondria from larger quantities of HeLa cells grown in suspension culture was conducted essentially as described (21). For smaller scale preparations from 2.0×10^8 HeLa or 3T3 cells grown in monolayer culture, a modification of the digitonin lysis method (26) was used. Cells were pelleted at $500 \times g$ for 5 min; washed with PBS and then with MIB (210 mM mannitol, 70 mM sucrose, 20 mM Hepes, pH 8.0, 2 mM EDTA, 2 mM DTT, and 0.2 mg/ml BSA); and resuspended in 3 ml of MIB. 8 μl of 10% digitonin was added, cell permeabilization to trypan blue was confirmed microscopically, and then 7 ml of MIB was added to dilute the digitonin. Cells were pelleted at $1200 \times g$, resuspended in MIB, and passed through a 25-gauge needle until cells were completely homogenized, usually eight times. Cell lysis was confirmed by microscopic inspection. 5 ml of MIB was added to the lysate, and the nuclei were removed by three sequential centrifugation steps at $900 \times g$ for 5 min each. Mitochondria were sedimented from the postnuclear supernatant by centrifugation in a Sorvall HB-6 swinging bucket rotor at $16,000 \times g$ for 15 min. For some experiments, mitochondria purified to this stage were used for protein or RNA preparation. In other experiments, the mitochondria were resuspended in 3 ml of MIB containing 1 M KCl to dissociate nucleic acids and cytoplasmic proteins adherent to mitochondria (27) and repelleted. Mitochondria were treated with DNase I and TurboNuclease as described (21) and then repelleted, resuspended in MIB lacking BSA, and centrifuged to the interface of a 1 M/1.7 M sucrose step gradient in buffer containing 20 mM Hepes, pH 8.0, 2 mM EDTA, 2 mM DTT, and protease inhibitors. Gradients were centrifuged at $112,000 \times g$ for 25 min at 4 °C in 14×89 -mm tubes in a swinging bucket rotor. Mitochondria were withdrawn from the interface and resuspended in three volumes of $0.5 \times$ MIB lacking BSA. The pure mitochondria were pelleted and frozen at -80 °C or directly lysed with Triton X-100 as reported below.

Mitochondrial Lysis and Preparation of Nucleoid and Ribosomal Fractions—Mitochondria were lysed with 2% Triton X-100 in 20 mM Hepes, pH 8, 20 mM NaCl, 2 mM EDTA, 2 mM DTT with protease inhibitors as above. Insoluble material was removed by centrifugation at $5000 \times g$ for 5 min at 4 °C, and 700 μl of soluble supernatant was layered over a 10-ml 15–40% glycerol gradient containing gradient buffer (20 mM NaCl, 10

mM Hepes, pH 8, with 0.2% Triton X-100 and protease inhibitors as above) with 2 mM EDTA formed over a pad containing 30% iodixanol, 20% glycerol in gradient buffer. The contents were centrifuged in 14×89 -mm tubes at $210,000 \times g$ for 4 h at 4 °C. Fractions were collected from the bottom of the gradient. Glycerol gradient fraction 1, containing nucleoids, and pooled fractions containing the peak of SYBR Green II RNA staining representing mitochondrial ribosomes (typically fractions 7–11) were separately analyzed by equilibrium centrifugation through 20–40% iodixanol in gradient buffer with 0.2% Triton X-100 and 2 mM EDTA at $140,000 \times g$ overnight at 4 °C. Fractions were collected from the bottom of the gradient. The ribosome-containing fractions were concentrated by ultrafiltration using a Vivaspin 50-kDa centrifugal concentrator prior to loading on iodixanol gradients. For higher resolution sedimentation analysis to separate 28 S and 39 S subunits from 55 S ribosomes, mitochondria were lysed in a buffer containing 10 mM Tris, pH 7.5, 100 mM KCl, 2% Triton X-100, 5 mM β -mercaptoethanol, and 20 mM MgCl_2 . The soluble fraction of the mitochondrial lysate was separated by spinning at $3000 \times g$ for 5 min at 4 °C and was then centrifuged through a 10-ml 10–30% sucrose gradient containing the same buffer as used to lyse the mitochondria, but with 0.02% Triton X-100 and either 20 mM MgCl_2 or 2 mM EDTA, over a pad of 30% glycerol, 30% iodixanol, for 17 h at $70,000 \times g$ at 4 °C. Smaller scale preparations were centrifuged in 11×60 -mm tubes.

Quantification of Nucleic Acids in Recovered Fractions—Samples of 5–10 μl of gradient fractions were mixed with 100 μl of 100 mM NaCl/TE buffer containing 1:2000 diluted SYBR Green I or II dye (for DNA or RNA) (Invitrogen) in 96-well microtiter plates, and fluorescence was detected using a Typhoon FLA 9000 imager.

Affinity Purification of FLAG-tagged RNMTL1—Mitochondrial pellets were resuspended in 150 μl of FLAG column wash buffer provided by Sigma supplemented with Triton X-100 and protease inhibitors (50 mM Tris, pH 7.4, 150 mM NaCl, 0.02% Triton X-100). An equal volume of $2 \times$ lysis buffer consisting of 100 mM Hepes, pH 7.5, 200 mM NaCl, 4% Triton X-100, and protease inhibitors was added, and the suspension was mixed gently by pipetting. The insoluble fraction was removed by centrifugation at $15,000 \times g$ for 5 min at 4 °C. FLAG-tagged RNMTL1 in the soluble fraction was recovered on FLAG M resin (Sigma-Aldrich) according to the manufacturer's protocol. Briefly, proteins were incubated with resin for 3 h at 4 °C while rotating, unbound proteins were removed by six successive washes with 200 μl of the provided wash buffer supplemented with 0.02% Triton X-100 and protease inhibitors, and the bound proteins were eluted with three incubations with 200 μl of 150 $\mu\text{g}/\text{ml}$ FLAG₃ peptide diluted in wash buffer. All of the handling was performed in a batch-wise format in a 0.6-ml microcentrifuge tube. The supernatants were separated from the resin by centrifugation at $1000 \times g$ for 1 min at 4 °C in a swinging bucket rotor.

Proteomics—A 20- μl sample of the eluate was boiled in standard Laemmli sample loading buffer for 5 min and briefly electrophoresed into a polyacrylamide gel. The gel was submitted to the Proteomics Center at Stony Brook University. Tryptic fragments were analyzed by LC-MS/MS using a Thermo

Fisher Scientific LTQ Orbitrap XL ETD mass spectrometer by matching collision-induced dissociation spectra against a library of known peptide spectra derived from the Swiss-Prot/Trembl database. Raw data were analyzed by the Inspect and Sequest programs and collated with Scaffold.

siRNA-directed Depletion of RNMTL1—HeLa cells were transfected with 3 or 6 nM silencer siRNA oligonucleotides directed against human RNMTL1 or with a scrambled negative control oligonucleotide using RNAiMax reverse transfection, as suggested by the supplier (Invitrogen), and RNA was isolated from total cells or from a partially purified mitochondrial fraction using TRIzol (Invitrogen). Alternatively, protein was isolated from partially purified mitochondria as described below. In some experiments, RNA was treated with DNase I and used to generate cDNA for real-time quantitative PCR (RT-PCR) analysis using kits obtained from Ambion (Invitrogen). RT-PCR was performed with SYBR Green I quantification using a Step One Plus instrument (Applied Biosystems) using primers derived from mtDNA sequences for 16 S rRNA (5'-CCAAAC-CCACTCCACCTTAC and 5'-TCATCTTCCCTTGCGG-TAC) and 12 S rRNA (5'-TAGATACCCCACTATGCTTAGC and 5'-CGATTACAGAACAGGCTCC) and mRNAs for ND1 (5'-TCAAACCTCAAACACTACGCCCTG and 5'-GTTGTGAT-AAGGGTGGAGAGG), ND2 (5'-CTACTCCACCTCAATC-ACACTAC and 5'-AGGTAGGAGTAGCGTGGTAAG), ND5 (5'-GTCCATCATAGAATTCTCAC and 5'-GCCCTCTCAG-CCGATGAAC), ND6 (5'-CCACAACCACCACCCCATC and 5'-GGTTGAGGTCTTGTTGAGT), and COXI (5'-ACACG-AGCATATTTACCTC and 5'-CCTAGGGCTCAGAGCAC-TGC). RT-PCR was also used under similar conditions to detect 12 S and/or 16 S rRNA in glycerol gradient fractions.

Mitochondrial Protein Synthesis—³⁵S labeling of mitochondrial proteins was performed essentially as described (28). HeLa cells transfected with siRNA oligonucleotides directed against RNMTL1 or a negative control scrambled sequence were cultured for 3 days. Cells were rinsed for 5 min with Hanks' balanced salt solution and then for 5 min with DMEM lacking cysteine and methionine and then for 5 min with the same depleted medium supplemented with dialyzed fetal bovine serum and 100 μg/ml emetine. After this pretreatment, 8 μl (~80 μCi) of [³⁵S]cysteine/methionine was added to 4 ml of medium for 1 h of labeling. This medium was then changed to complete DMEM with 10% fetal bovine serum for a 30-min chase in the continued presence of emetine. Partially purified mitochondria were prepared as described above. Incorporation was analyzed by TCA precipitation and scintillation counting or by SDS-PAGE. Coomassie Blue-stained gels were dried, and incorporation was quantified using a Typhoon 9000 imager (GE Healthcare).

Primer Extension to Identify 2'-O-Methyl Blocking Residues—Cells transfected with siRNA oligonucleotides or with negative control scrambled oligomers were used to prepare crude mitochondrial fractions. RNA was prepared from partially purified mitochondria using TRIzol. To provide a control unmodified RNA sequence, T7 RNA polymerase (Ambion T7 Megascript) was used to transcribe a recombinant version of human 16 S rDNA obtained from Edison Mejia and Miguel Garcia-Diaz (Stony Brook University). Oligonucleotide primers were syn-

thesized with sequences having 3'-termini 4 or 5 nucleotides away from known 2'-O-ribose modification sites in domain 5 (5'-GGTTGGGTTCTGCTCCGAGG) or domain 6 (5'-GAT-CACGTAGGACTTTAATCG) of human 16 S rRNA. Primers were labeled at 5'-termini using [γ -³²P]ATP and polynucleotide kinase and were purified by electrophoresis on urea-14% polyacrylamide gels. Labeled primers were annealed to 500 ng of crude mtRNA or T7 transcript in first strand buffer for Superscript 3 reverse transcriptase (Invitrogen). The annealed mixture was supplemented with Superscript 3 reverse transcriptase, RNasin RNase inhibitor, and dithiothreitol and then aliquoted to reactions containing varied concentrations of all four dNTPs for 30 min of extension at 37 °C. Reactions were terminated by the addition of 0.3 M sodium acetate, 20 mM EDTA, and 10 μg of glycogen carrier. Nucleic acids were ethanol-precipitated, boiled in formamide loading solution containing 10 mM EDTA, and analyzed by electrophoresis on urea-14% polyacrylamide DNA sequencing gels. Radioactivity was detected using a Typhoon 9000 PhosphorImager.

UV Cross-linking of [³H]AdoMet to Proteins—UV cross-linking was performed essentially as described (29) in a buffer containing 50 mM Tris-HCl, pH 8.0, 40 mM NaCl, 2 mM DTT, 2 mM EDTA, and 1.1 μCi of [³H]AdoMet. 10-μl reactions containing BSA (14.5 pmol), RNMTL1 (14.2 pmol), MRM1 (51 pmol), MRM2 (49 pmol), or MTERF4-NSUN4 complex (3.8 pmol) were assembled, incubated on ice for 10 min, and then spotted onto a siliconized microscope slide. The slide was placed on ice and exposed to 254-nm UV light for the indicated times, and then the samples were collected, boiled in sample loading buffer, and subjected to electrophoresis on an SDS-polyacrylamide gel. The gel was stained and destained with Coomassie Blue and then soaked in AmplifyTM (Amersham Biosciences) for 45 min, dried onto 3MM Whatman paper, and exposed to x-ray film at -80 °C.

RESULTS

Mitochondrial Methyltransferase Family Members—Our identification of RNMTL1 and of RG9MTD1 (MRPP1 (30)) in association with mitochondrial nucleoids stimulated a search for other mitochondrial members of the RNA methyltransferase family. We noted that mammalian genomes contain two putative mitochondrial members of the SPOUT family of methyltransferases, RNMTL1 and MRM1, both of which contain 2'-O-ribose binding sites and SPOU methylase domains (Fig. 1A) as well as MRM2, a protein not previously shown to reside in mitochondria, as noted in the Introduction. We analyzed these putative mitochondrial methyltransferases by multiple-sequence alignment along with the established methyltransferase family members mouse TFB1M and TFB2M, yeast PET56p/MRM1, yeast MRM2, and *E. coli* KsgA and RLME (Fig. 1B). This analysis revealed that RNMTL1 clusters closely with mammalian MRM1 and yeast PET56p, whereas mammalian MRM2 clustered with yeast MRM2 and *E. coli* RLME (FtsJ). MRM2 is thus a strong candidate for the enzyme activity that modifies the U¹³⁶⁹ site in human 16 S rRNA. We also confirmed that RNMTL1, MRM1, and MRM2 are enriched in a mitochondrial fraction from HeLa cells (Fig. 1, C-E). Our bioinformatic search revealed an additional RNA methyltransferase member,

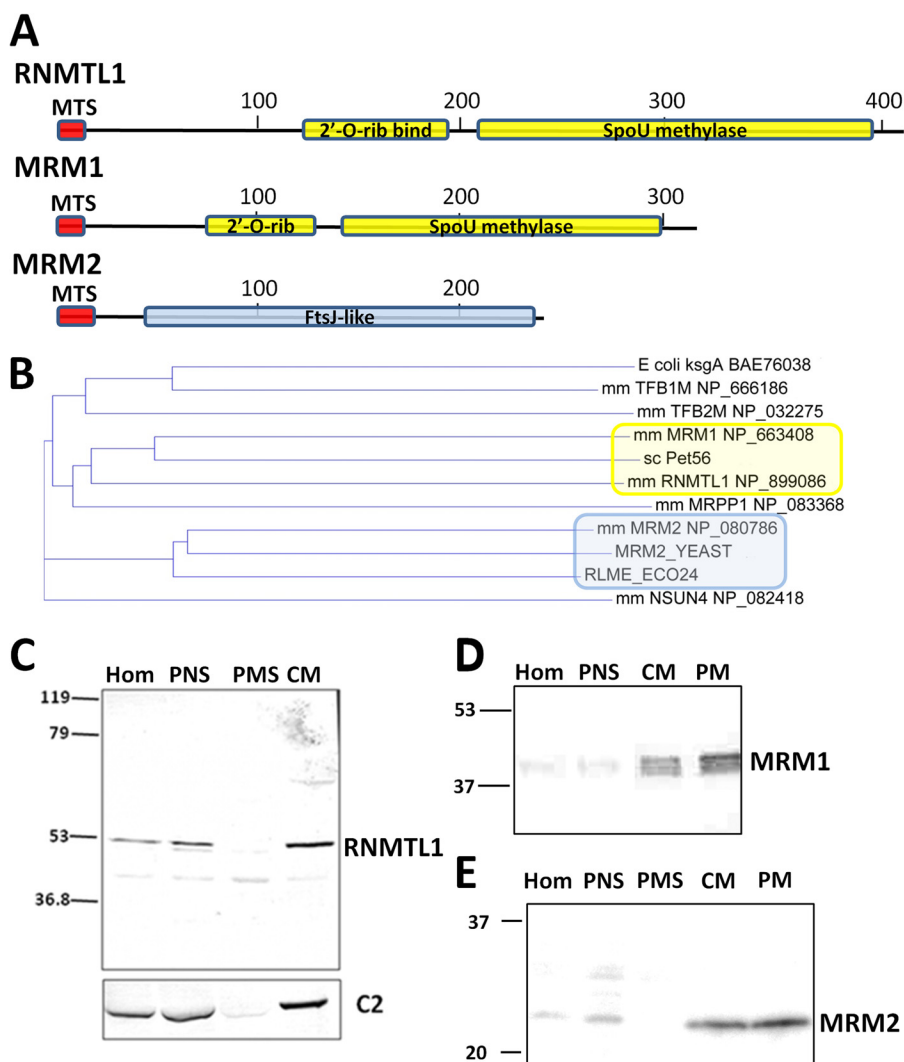


FIGURE 1. RNMTL1 is a mitochondrial member of the methyltransferase family. *A*, human (420 amino acids, NP_060616) and mouse (418 amino acids, NP_899086) RNMTL1 are 86% identical and share a general organization with mouse MRM1 (320 amino acids, NP_663408), which features a SPOU-like methyltransferase domain following a 2'-*O*-methyl-ribose binding site. Mouse MRM2 (246 amino acids, NP_080786) is also diagrammed. Only the mouse proteins are shown. *B*, dendrogram showing sequence relationships revealed by multiple alignment of seven mouse mitochondrial proteins with features of methyltransferases along with *E. coli* methyltransferases KsgA and RLME_ECO24 (FtsJ/RrmJ), responsible for the U²⁵⁵² methylation (62) and *Saccharomyces cerevisiae* PET56 and MRM2. The yellow box indicates that mouse RNMTL1 and MRM1 cluster with PET56. The blue box indicates that MRM2 clusters with yeast MRM2 and *E. coli* RLME. *C*, immunoblots of HeLa cell fractions (10 μ g/lane) for RNMTL1 and a positive control for the 70-kDa SDHA subunit of mitochondrial respiratory complex II (C2). *D* and *E*, enrichment of MRM1 (*D*) and MRM2 (*E*) in purified mitochondria. *Hom*, total homogenate; *PNS*, postnuclear supernatant; *PMS*, postmitochondrial supernatant; *CM*, crude mitochondria; *PM*, pure mitochondria, after the sucrose gradient step.

FtsJ3 (NP_079586), with a strong mitochondrial localization signal (98% probability of mitochondrial import using Mitoport). This protein is extensively annotated as a nucleolar protein and was not considered further at this time. It is conceivable that this protein may have dual localization in mitochondria and nucleoli.

Mitochondrial Localization of Novel Methyltransferase Members—The mitochondrial localization of TFB1M, TFB2M, MRPP1, and NSUN4 is well established. To investigate the localization of RNMTL1, MRM1, and MRM2 in cells, we cloned the cDNAs encoding these proteins fused to a C-terminal Eos fluorescent reporter in a derivative of the pGS vector (31). We transfected the plasmids into 3T3-Switch cells and selected stable transformants that permit controlled expression of the proteins upon the addition of mifepristone. The C-terminal fluorescent protein tag in these experiments permitted us

to confirm that all three proteins contain N-terminal localization sequences that deliver the fusion proteins to mitochondria, visualized with MitoTracker Red or with immunofluorescence localization of a mitochondrial protein, SDHA (Fig. 2, *A*, *C*, and *E*). Our results with MRM2 contrast with those of Ching *et al.* (23), who found that fusion of the protein to an N-terminal fluorescent reporter concealed an N-terminal mitochondrial targeting signal and permitted the fusion protein to enter nuclei. Similar misrouting resulting from a buried mitochondrial targeting signal has been observed occasionally in other studies. Although we saw no evidence of nucleolar localization of the MRM2 fusion protein, we cannot rule out the possibility that some of the protein may enter nuclei in some cell types. For each of our methyltransferase family member constructs, the fluorescent fusion proteins did not fill the mitochondrial matrix but formed punctate foci similar to mtDNA nucleoids. We per-

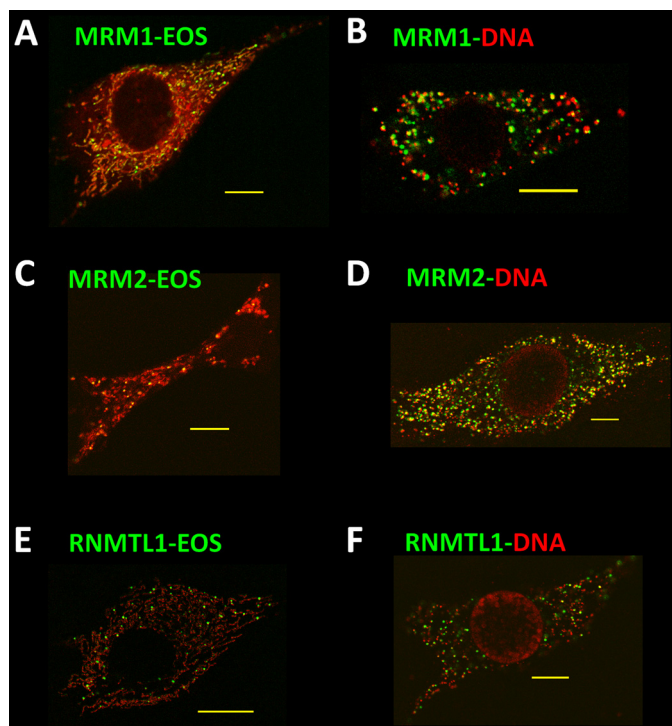


FIGURE 2. Methyltransferase family members direct a fluorescent reporter protein to mouse mitochondria. *A*, 3T3-Switch cells expressing MRM1-Eos (green) were incubated with 50 nM MitoTracker Red (red) for 1 h to visualize mitochondria. *B*, fixed cells expressing MRM1-Eos were incubated with anti-DNA primary antibodies and Alexa 568-conjugated secondary antibodies (red). *C* and *D*, MRM2-Eos-expressing cells were processed as in *A* and *B*, respectively. *E*, RNMTL1-Eos-expressing cells were decorated with mouse anti-complex II (70 kDa) primary antibody and an Alexa 568-conjugated goat-anti-mouse antibody (red). *F*, RNMTL1-Eos-expressing cells were stained with anti-DNA antibodies (red) as in *B* and *D*. Scale bars, 10 μ m.

formed a second set of indirect immunofluorescence imaging experiments in which we visualized mtDNA by applying an anti-DNA antibody (Fig. 2, *B*, *D*, and *F*). All three putative mammalian mitochondrial methyltransferases were localized in the vicinity of nucleoids, consistent with their proposed function in methylating 16 S rRNA transcribed from mtDNA.

Because we were particularly interested in RNMTL1, we probed human HeLa cells with a commercial RNMTL1 antibody that recognizes a sequence conserved in both human and mouse proteins (Fig. 3*A*). The resulting immunostaining pattern revealed that the endogenous RNMTL1 is also localized in punctate foci. Similar immunofluorescence with 3T3 cells is shown in Fig. 3*B* with additional anti-DNA antibody staining to document that the endogenous protein is located near nucleoids. We were not able to obtain adequate results with indirect immunofluorescence for MRM1 and MRM2 because the antibodies we used for immunoblotting did not give satisfactory results in immunofluorescence.

Fractionation of Mitochondrial Contents in a Glycerol Gradient Reveals RNMTL1 Co-sedimentation with Nucleoids and Ribosomes—To determine whether RNMTL1 exists in a macromolecular complex, purified HeLa mitochondria were lysed with 2% Triton X-100, and the soluble contents were loaded onto a 15–40% glycerol gradient containing 0.2% Triton X-100 and 2 mM EDTA. The continuous presence of non-ionic detergent in these gradients during sedimentation assures that pro-

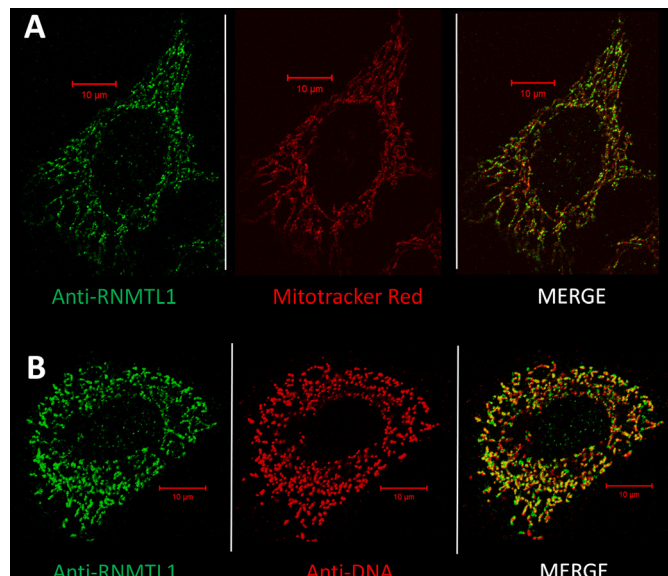


FIGURE 3. Submitochondrial localization of endogenous RNMTL1 in mammalian mitochondria. *A*, rabbit-anti-RNMTL1 primary and Alexa 488-labeled goat-anti-rabbit antibodies (green) were used to identify RNMTL1 in HeLa cell mitochondria stained with MitoTracker Red (red). *B*, RNMTL1 indirect immunofluorescence as in *A* combined with mouse monoclonal anti-DNA antibodies and Alexa 568-conjugated goat anti-mouse secondary antibodies (red) in mouse 3T3 cells. Scale bars, 10 μ m.

teins are effectively solubilized. Fraction 1 contains nucleoids, as identified by mtDNA analysis and TFAM content (data not shown), that sedimented onto a pad of 20% glycerol, 30% iodixanol (Fig. 4). Due to the presence of EDTA, these gradients are expected to dissociate ribosomes to small and large ribosomal subunits. The fractions containing MRPL13 protein (measured by immunoblot densitometry) and 16 S rRNA (measured by quantitative PCR) are shown as markers for 39 S subunits (Fig. 4). Each fraction was immunoblotted for RNMTL1 (*panel above the graph*). It is apparent that RNMTL1 exists in two complexes that co-sediment with nucleoids and ribosomes, respectively. A second preparation prepared under the same conditions was used for immunoblot localization of MRM1 and MRM2 (Fig. 4*B*). Whereas MRM1 was found in the rapidly sedimenting fraction, the second major proportion of protein was not enriched in the ribosome-containing fractions but resided near the top of the gradient with the majority of free proteins or small complexes. In contrast to these, MRM2 was not enriched in the nucleoid fraction but did co-sediment with ribosomes or other large structures. MRPL13 was only barely detectable in the rapidly sedimenting nucleoid fraction (Fig. 4*A*). These results are consistent with the hypothesis that RNMTL1 and MRM1 may interact with nascent mitochondrial transcripts that have not yet dissociated from the DNA template, whereas MRM2 may function later.

Buoyant Density Gradients Support the Existence of Two RNMTL1 Complexes—To determine whether the proteins that co-sedimented with nucleoids, RNMTL1 and MRM1, are stably associated with the nucleoid, fraction 1 of the glycerol gradient was loaded on a non-ionic buoyant density gradient containing iodixanol (Optiprep) that fractionates macromolecules by density, not simply by sedimentation coefficient. We have used similar gradients containing metrizamide to characterize

RNA Methyltransferase Family Members at mtDNA Nucleoids

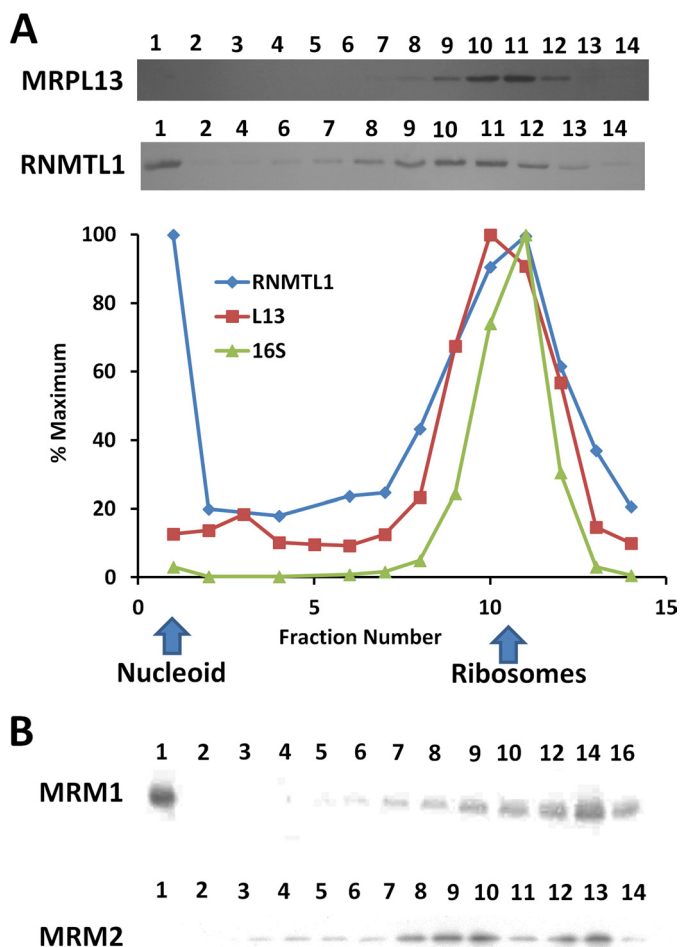


FIGURE 4. Glycerol gradient sedimentation reveals RNMTL1 in rapidly sedimenting complexes consistent with association with mtDNA nucleoids and mitochondrial ribosomes. *A*, a detergent lysate of HeLa cell mitochondria was fractionated by sedimentation through a 15–40% glycerol gradient for 4 h in the presence of 2 mM EDTA and 0.2% Triton X-100. Immunoblots for MRPL13 and RNMTL1 in the gradient fractions are shown. These signals were quantified by densitometry to compare sedimentation of the proteins with that of 16 S rRNA detected by quantitative RT-PCR in the graph. Note that individual fractions were omitted in some cases. *B*, immunoblots showing the sedimentation of MRM1 and MRM2 in an independent glycerol gradient experiment performed under the same conditions as in *A*.

Xenopus mtDNA nucleoids previously (32). Nucleoids were identified in the buoyant density gradient by their content of DNA, determined by SYBR Green I fluorescence, and the presence of the abundant DNA-binding protein TFAM. Fractions surrounding the SYBR Green I-stained peak were extracted with phenol-CHCl₃ and digested with HindIII to confirm the presence of mtDNA (Fig. 5*A*). Both RNMTL1 and MRM1 were identified in fractions containing mtDNA and TFAM (Fig. 5*B*). Ribosomes and free proteins are found at lower densities, closer to the top of such gradients. This suggests that the two methyltransferase proteins may modify newly synthesized rRNA while it is still being transcribed, as is known to occur during ribosome assembly in bacteria and in eukaryotic nucleoli.

Although we found that both RNMTL1 and MRM1 associate firmly with nucleoids, the two proteins behaved differently in the glycerol gradient in Fig. 4. RNMTL1, like MRM2, appeared to co-sediment with ribosomes, whereas the fraction of MRM1 not associated with nucleoids behaved as a free protein. The

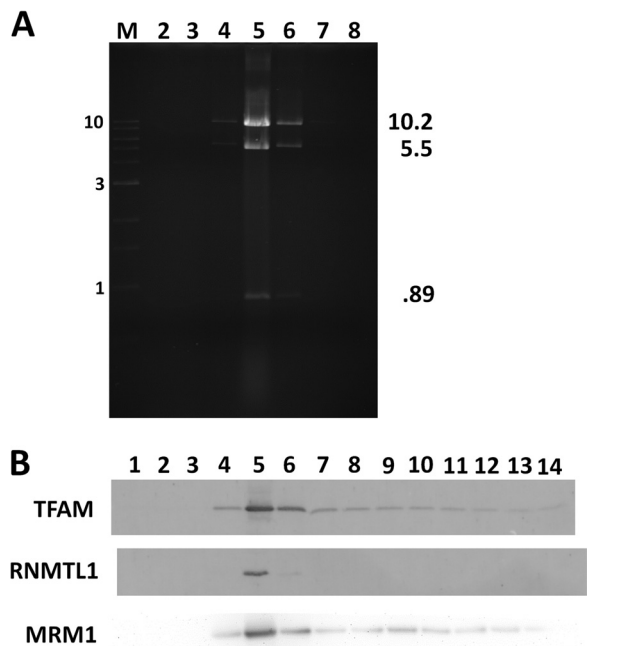


FIGURE 5. RNMTL1 and MRM1 sedimenting with the nucleoid fraction remain associated with nucleoids following equilibrium centrifugation in an iodixanol gradient. *A*, fraction 1 from the glycerol gradient in Fig. 4 was centrifuged on a 20–40% iodixanol gradient as described under “Experimental Procedures.” Fractions were collected from the tube bottom and assayed for the presence of DNA by monitoring SYBR Green I fluorescence. Fractions surrounding the fluorescent peak were extracted, and the DNA was digested with HindIII restriction endonuclease to confirm the positions of mtDNA nucleoids. Sizes of human mtDNA HindIII fragments are shown on the right in kb. Selected bands from the 1 kb marker ladder are labeled on the left. *B*, RNMTL1 and MRM1 were detected by SDS-PAGE and immunoblotting in the indicated fractions from the iodixanol gradient with TFAM serving as a nucleoid marker.

apparent association of RNMTL1 and MRM2 with ribosomes was unexpected because the proteins are expected to dissociate from ribosome assembly intermediates after completing the task of modifying the RNA. We used isopycnic centrifugation to further study the apparent persistent association of RNMTL1 and MRM2 with ribosomes. The glycerol gradient fractions that were enriched in ribosomes were pooled, concentrated by ultrafiltration, and centrifuged to equilibrium in a 20–40% non-ionic iodixanol gradient similar to that used to study nucleoids. RNMTL1 and MRM2 were enriched in gradient fractions containing ribosomal complexes identified by SYBR Green II RNA fluorescence as well as immunoblotting for MRPS15 and MRPL13 markers (Fig. 6). The buoyant density of ribosomes in such gradients depends on their content of both protein and RNA. Because only the 16 S rRNA contains 2'-*O*-ribose modifications, we considered it likely that RNMTL1 and MRM2 were specifically associated with the large ribosomal subunit. However, the glycerol gradient shown in Fig. 4 was only centrifuged for 4 h to permit recovery of both nucleoids and ribosomes. Therefore, we performed a second sedimentation velocity experiment using 10–30% sucrose gradient sedimentation in buffer containing 20 mM MgCl₂ to stabilize 55 S ribosomes and for a longer interval to permit separation of large and small mitochondrial ribosomal subunits. Under these conditions, RNMTL1 co-sedimented with MRPL13 in 39 S subunits rather than with MRPS15 in 28 S subunits, as was confirmed by quan-

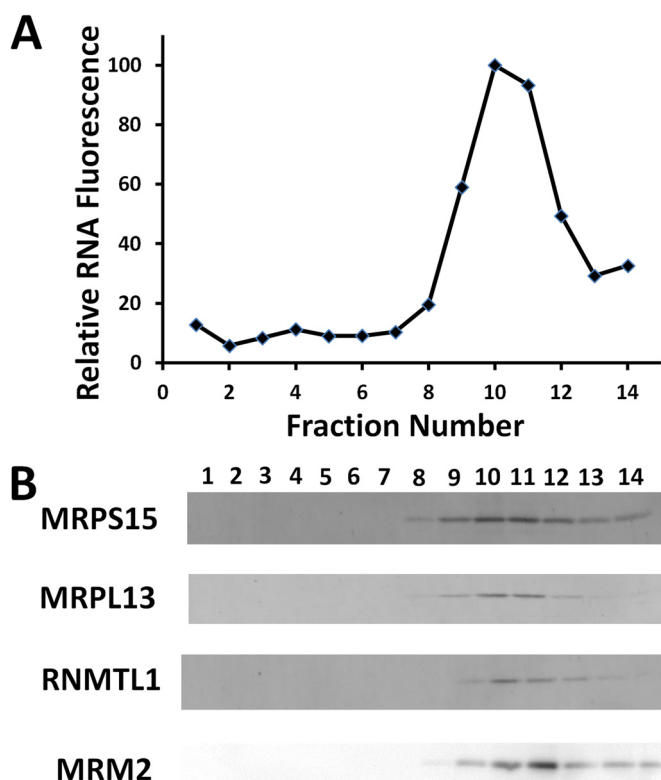


FIGURE 6. RNMTL1 sedimenting in glycerol gradient fractions enriched in ribosomes remains associated with ribosomes following equilibrium centrifugation in an iodixanol gradient. *A*, fractions 8–11 from the glycerol gradient in Fig. 4 enriched in ribosomes were centrifuged as in Fig. 5. Fractions were collected from the tube bottom and assayed for the presence of RNA by monitoring SYBR Green II fluorescence. *B*, RNMTL1 and MRM2 were detected by SDS-PAGE and immunoblotting. MRPS15 and MRPL13 are markers for subunits of the small and large mitochondrial ribosomes, respectively.

titative PCR of 12 S and 16 S rRNA levels in fractions 12–25 (Fig. 7, *A* and *B*). Interestingly, MRM2 sedimented as a free protein in the presence of 20 mM MgCl₂, suggesting that its association with the ribosomal subunits in Figs. 4 and 6 is salt-sensitive. Additionally, low levels of MRM1 were detected in higher molecular weight complexes throughout fractions 15–28 upon long exposure (*MRM1 (hi)*).

Identification of Proteins Complexed with RNMTL1—To gain further insight into the molecular partners of RNMTL1, we cloned mouse RNMTL1 in the pGS-3FH vector to provide a C-terminal FLAG₃-His₆ tag and stably transfected this plasmid into 3T3-Switch cells. Mitochondria were isolated from ~2 × 10⁸ cells after mifepristone induction and lysed in 2% Triton X-100, and the soluble proteins were immunopurified on FLAG M resin. No magnesium or EDTA was added to the buffers in handling this lysate. A silver-stained SDS-PAGE analysis of the FLAG eluate revealed numerous small proteins characteristic of ribosomes (Fig. 8) (see below). A sample of the eluate was briefly electrophoresed into a 10% SDS-polyacrylamide gel and submitted to the Proteomics Facility at Stony Brook University. This experiment was conducted twice, first with crude sucrose gradient purified mitochondria and later with mitochondria washed with a buffer containing 1 M KCl to release proteins and nucleic acids adherent to the outer surface of mitochondria, including cytoplasmic ribosomes (27). We confined our analy-

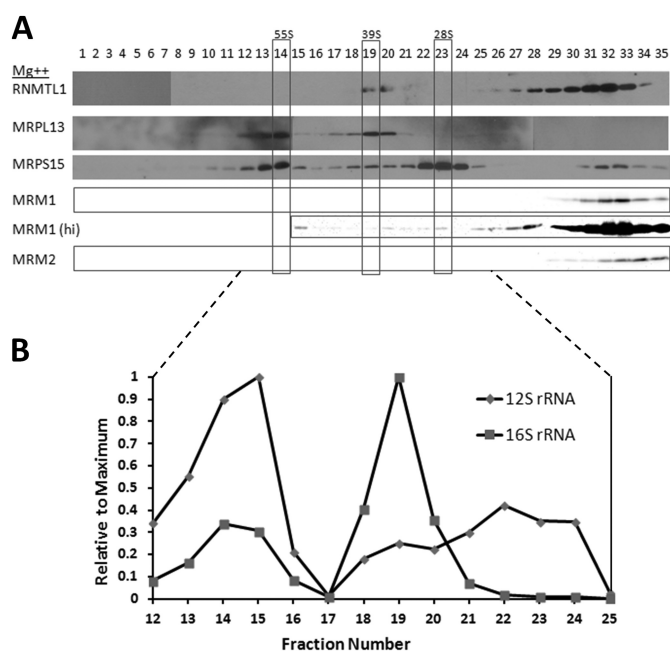


FIGURE 7. RNMTL1 associates with the 39 S large ribosomal subunit in sucrose gradients in the presence of Mg²⁺. *A*, sedimentation of a HeLa mitochondrial lysate through a 10–30% sucrose gradient containing 20 mM MgCl₂ to permit resolution of the 28 S and 39 S subunits from intact 55 S mitoribosomes. The indicated proteins were identified by immunoblotting; the chemiluminescence was detected by film (RNMTL1, MRPL13, and MRPS15) or by a CCD camera (MRM1 and MRM2). *B*, quantitative PCR of fractions 12–25 for 12 S and 16 S rRNA supports identification of the monosome and large and small ribosomal subunits in *A*.

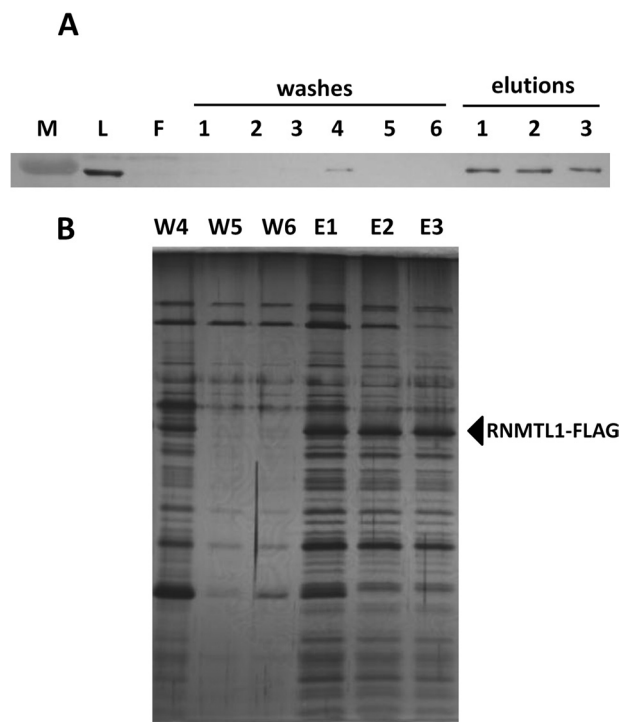


FIGURE 8. Affinity chromatography purification of FLAG-tagged RNMTL1. Mitochondria were isolated from 3T3-Switch cells expressing mouse RNMTL1-FLAG₃-His₆. *A*, anti-FLAG immunoblot analysis of fractions obtained during immunopurification on an anti-FLAG antibody column showing the lysate (*L*), the column flow-through (*F*), six successive washes, and three successive elutions with wash buffer containing FLAG peptide. *Lane M* contains one of a series of prestained mobility markers. *B*, silver-stained SDS-12% PAGE of the three final wash fractions and the first three fractions eluted from the FLAG affinity column.

TABLE 1
Non-ribosomal mitochondrial proteins eluted with RNMTL1-FLAG

Non-ribosomal mitochondrial proteins	Accession no.	Molecular mass	Spectral counts	
			Experiment 1	Experiment 2
		<i>kDa</i>		
RNMTL1	RMTL1_MOUSE	47	44	28
LRPPRC	LPPRC_MOUSE	157	11	18
Probable ATP-dependent RNA helicase DDX28	DDX28_MOUSE	60	14	8
HSP60 (Hspd1)	CH60_MOUSE	61	3	18
HSP75	GRP75_MOUSE	73	1	19
P32, C1qbp	Q8R5L1_MOUSE	31	2	10
RPUSD4	RUSD4_MOUSE	42	7	3
PTCD3	PTCD3_MOUSE	78	0	9
G-rich sequence factor 1 (GRSF1)	E9Q179_MOUSE	42	2	6
SQRDL	SQRD_MOUSE	50	4	4
mTERF3 (Mterfd1)	MTER1_MOUSE	47	0	7
DNA-directed RNA polymerase POLRMT	E9PWD9_MOUSE	128	3	2
Leucine-rich repeat protein 59 LRRC59	LRC59_MOUSE	35	3	2

sis to proteins that remained well represented following this salt wash step.

Over half of the immunoprecipitated proteins were mitochondrial ribosomal proteins, including 170 spectra of 14 large subunit proteins and 37 spectra representing six small subunit proteins. This distribution reflects the preferential association of RNMTL1 with the 39 S subunit in sedimentation experiments. We also observed a significant number of spectra derived from 12 non-ribosomal mitochondrial proteins, including mtRNA polymerase and MTERF3 as well as RNA-binding proteins LRPPRC, GRSF1, p32/C1QBP, and PTCD3, which has recently been proposed to be a ribosomal protein (33) (Table 1). Further experiments will be required to determine if these proteins interact directly with RNMTL1 or if they are simply components of a larger complex associated with the bait protein.

RNMTL1 Is Required for Mitochondrial Translation—To further characterize the *in vivo* role of RNMTL1, we used silencer-select modified siRNA to down-regulate the mRNA and protein. We used two siRNA reagents designated as R1 and R3 in Fig. 9 most extensively. Treatment with 3 or 6 nM siRNA for R1 or R3 resulted in a 90% reduction of RNMTL1 protein (Fig. 9A) but did not drastically alter the quantity of the mitochondrial rRNAs or of several mRNAs (Fig. 9B). Cells incubated with either siRNA reagent exhibited slower growth rates. We selected siRNA R1 for further tests because of its efficiency and tolerable toxicity. After 2–3 days of incubation with siRNA R1, incorporation of ³⁵S-labeled amino acids into mitochondrial protein during pulse labeling was decreased to ~40% of control labeling (*n* = 3) observed when a scrambled siRNA was used (Fig. 9C). We conclude that down-regulation of RNMTL1 leads to impaired mitochondrial protein synthesis.

We also sought to determine whether down-regulation of RNMTL1 would lead to a reduction in 2'-*O*-ribose modification of 16 S rRNA at previously characterized sites in domain 5 (Gm¹¹⁴⁵) or domain 6 (Um¹³⁶⁹Gm¹³⁷⁰) of the RNA secondary structure. Unfortunately, the most obvious way to study this modification by using *in vivo* methylation with radioactive S-[³H]adenosylmethionine was not practical due to the large quantity of isotopes used in such studies (6) and the limited amount of RNA available from siRNA knockdown specimens. As an alternative, we elected to use the method described by Maden *et al.* (34), who showed that 2'-*O*-ribose modification of

RNA created a block to extension of a radioactive primer by reverse transcriptase at low dNTP concentrations. In this method, a labeled oligonucleotide is annealed to RNA sequences on the 3'-side of a presumed modification site, and the extension of the primer by reverse transcriptase is tested in reactions in which the dNTP concentrations are varied. We found that application of this method to the two modification sites in 16 S rRNA was complicated for several reasons. First, in domain 5, we found that RNA secondary structures involving the GGGG sequence containing the Gm residue created a substantial block to extension by reverse transcriptase even when unmodified *in vitro* transcribed 16 S rRNA was used as template (Fig. 10, A and B). At this site, we observed an additional pause site just beyond the block created by the RNA secondary structure. Our results are consistent with the extension of the primer through residue 1146 of 16 S rRNA with a relative block at residue 1145. This impediment to primer extension was not affected when the assays used mtRNA purified from cells in which RNMTL1 was depleted. Second, at domain 6, the utility of the primer extension assay was influenced by the fact that the Um¹³⁶⁹ modification is immediately adjacent to the Gm¹³⁷⁰ modification. Unlike the situation in domain 5, we found that reverse transcriptase reads through this region readily when *in vitro* transcribed 16 S rRNA is used as template (data not shown). When HeLa mtRNA was used as template, this pair of modified residues blocks reverse transcriptase rather effectively at low dNTP concentrations. We observed a partial alleviation of the block at Gm¹³⁷⁰ in our experiments when RNMTL1 was down-regulated. A partial effect is expected because ribosomes assembled prior to onset of down-regulation are still present at the time of cell harvest. Furthermore, the results appear to be influenced by the close spacing between the adjacent methylation sites. Therefore, we can only tentatively conclude that down-regulation of RNMTL1 influences RNA methylation at residue G¹³⁷⁰.

As another approach to study the activity of RNMTL1 as well as MRM1 and MRM2, we expressed the mature forms of all three proteins lacking their presumed mitochondrial localization signals in bacteria using the T7 expression system. In pilot studies, we found that it was necessary to wash the RNMTL1 extensively with 1 M KCl while it was bound to the HisTrap affinity column in order to remove associated bacterial RNA. All three proteins were purified to near homogeneity (Fig. 11A) and found to elute from an analytical gel filtration column at

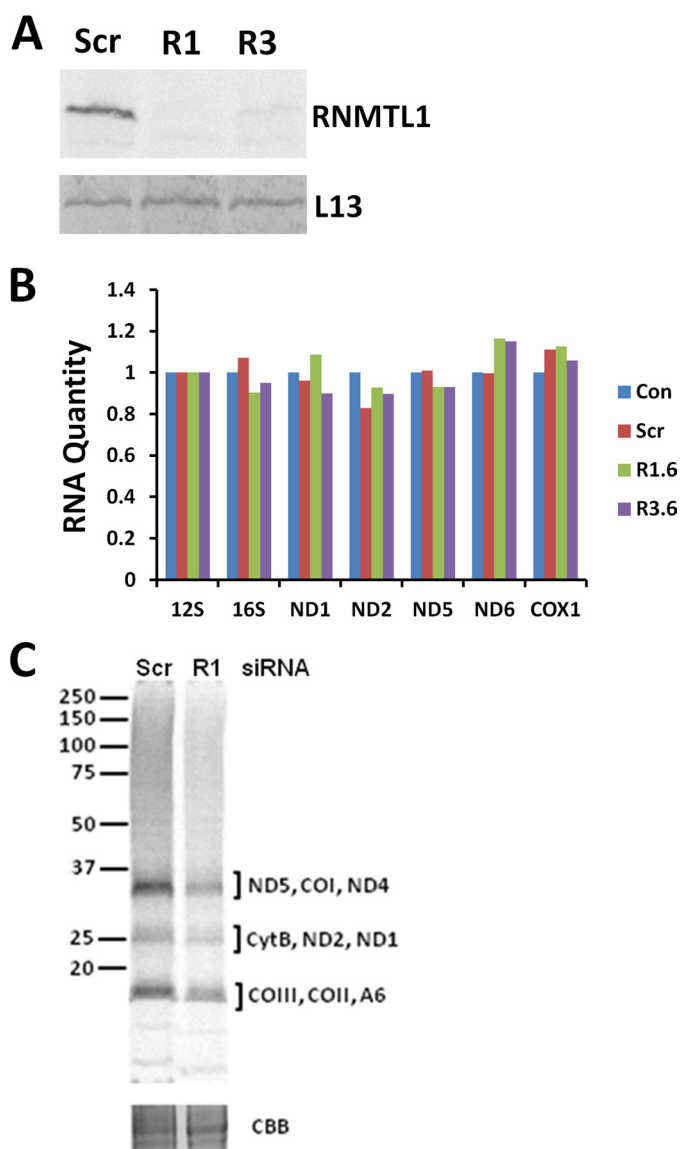


FIGURE 9. Down-regulation of RNMTL1 leads to impaired mitochondrial translation. *A*, HeLa cells were treated with a control scrambled siRNA (*Scr*) or with either of two siRNAs directed against RNMTL1 (*R1* and *R3*). Immunoblots were used to detect RNMTL1 and MRPL13, which served as a loading control. *B*, relative quantity of mitochondrial rRNAs and mRNAs detected by RT-PCR in samples generated using HeLa cells mock-transfected (*Con*) or transfected with a negative control scrambled siRNA (*Scr*) or 6 nM RNMTL1 *R1* or *R3* siRNAs (*R1.6* and *R3.6*). *C*, SDS-PAGE analysis of ^{35}S -labeled mitochondrial protein labeled in cells transfected with scrambled siRNA (*Scr*) or RNMTL1 siRNA *R1* (*R1*). A portion of the Coomassie Blue (*CBB*)-stained gel is shown below as a loading control.

positions consistent with monomeric quaternary structures (data not shown). This result was somewhat surprising because many RNA methyltransferases have been found to occur as dimers; in fact, all currently characterized SpoU methyltransferases exist as dimers (35). In experiments performed to date, we did not find convincing RNA methylation activity with any of these proteins while using *in vitro* transcribed human 16 S rRNA as substrate. To determine whether our purified proteins retained a functional AdoMet-binding pocket, we incubated them with [^3H]AdoMet and exposed them to UV light for various lengths of time. Bovine serum albumin (BSA), the negative control, did not cross-link to *S*-adenosylmethionine, whereas

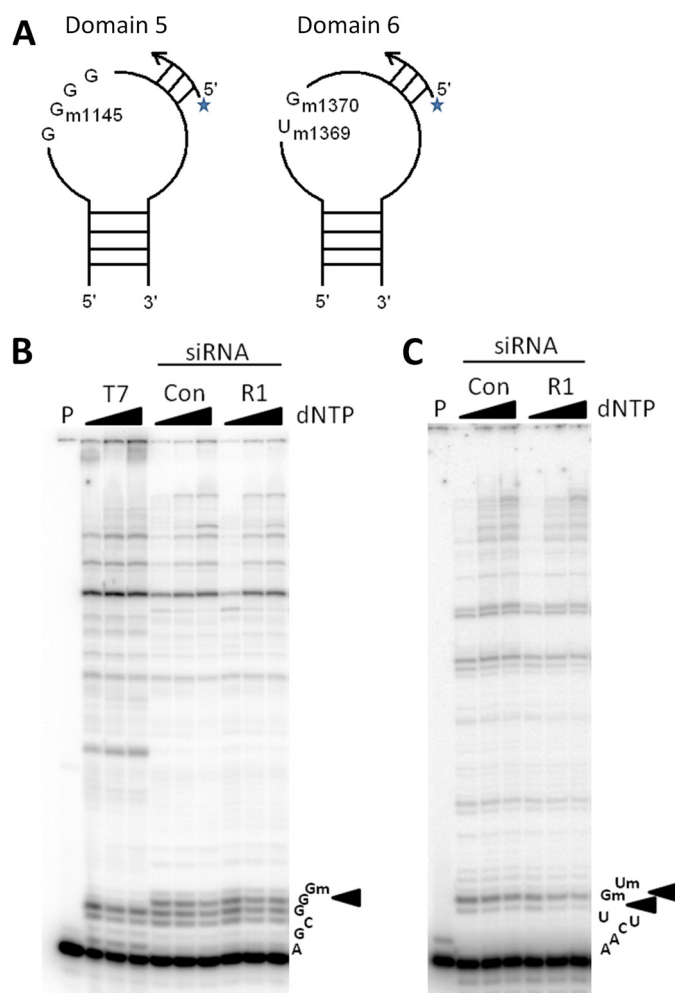


FIGURE 10. RNMTL1 down-regulation affects reverse transcriptase extension through Gm¹³⁷⁰ in domain 6 of 16 S rRNA. *A*, schematic diagram showing the orientation of primers with respect to known 2'-*O*-ribose modification sites in 16 S rRNA in domains 5 and 6 of the RNA secondary structure. *B*, primer extension analysis of Gm¹¹⁴⁵ read-through in domain 5. Products of primer extension using as template *in vitro* synthesized 16 S rRNA lacking modifications (*T7*) or crude mtRNA from cells exposed to scrambled control siRNA (*Scr*) or RNMTL1 *R1* siRNA for 3 days (*R1*) are shown for reactions at 2, 4, or 6 nM dNTPs. Lane *P* shows the mobility of the labeled primer. Labels at the bottom right show nucleotides encountered in the template during early extension. *C*, analysis similar to that shown in *B* but using a primer that annealed adjacent to Um¹³⁶⁹Gm¹³⁷⁰. *T7*-synthesized RNA was not used as template in these reactions because no prematurely terminated products were observed in the region of interest. Note that in these assays, a block to primer extension is observed as a band before the indicated template base.

NSUN4, the positive control, did cross-link, consistent with the recent report of its *in vitro* RNA methyltransferase activity (36). We found that MRM2, but not RNMTL1 or MRM1, also cross-linked to AdoMet (Fig 11, *B* and *C*). MRM1 and RNMTL1 are thought to resemble Pet56p in having an *S*-adenosylmethionine binding pocket with a deeply knotted structure distinct from that of MRM2 or *E. coli* RLME. At this point, we cannot be certain that our recombinant RNMTL1 or MRM1 proteins folded correctly when expressed in bacteria. If any of these proteins require additional factors to stabilize them, as seems to be the case for NSUN4-MTERF4 (19, 36, 37), these partners have not yet been identified. Because none of the mammalian mitochondrial RNA methyltransferase members we have expressed have robust RNA methyltransferase activity, it is also possible

RNA Methyltransferase Family Members at mtDNA Nucleoids

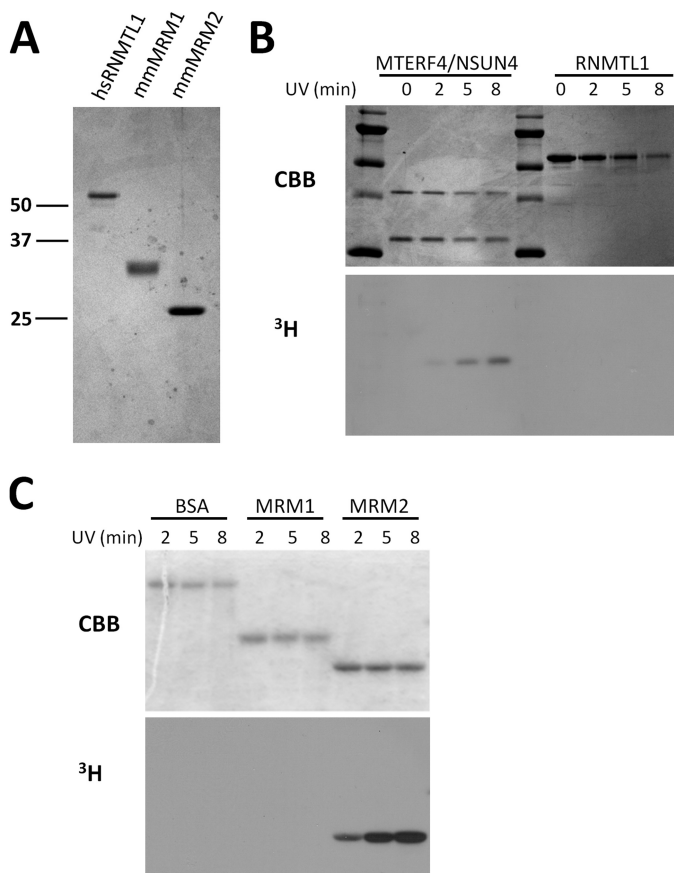


FIGURE 11. Recombinant RNMTL1 and MRM1 are not cross-linked to [³H]AdoMet under conditions that permit cross-linking for NSUN4 and MRM2. A, 500 ng of each of several purified recombinant proteins, human RNMTL1 (*hsRNMTL1*), mouse MRM1 (*mmMRM1*), and mouse MRM2 (*mmMRM2*) lacking their predicted mitochondrial localization signals, were separated on an SDS-12% polyacrylamide gel and stained with Coomassie Blue. B, recombinant MTERF4-NSUN4 (3.48 pmol) or RNMTL1 (14 pmol) proteins were preincubated with [³H]AdoMet and exposed to UV light for the indicated lengths of time. The samples were collected, boiled in sample loading buffer, and separated on an SDS-12% polyacrylamide gel and then analyzed by Coomassie Blue (CBB) and fluorography (³H). C, BSA (14.5 pmol) serving as a negative control, MRM1 (51 pmol), and MRM2 (49 pmol) were also tested for their ability to cross-link to AdoMet.

that they may act not on free 16 S rRNA but on RNA-protein complexes that are intermediates in ribosome assembly, as is the case for yeast MRM2 (18). Additional experiments beyond the scope of our present work will be required to confirm and characterize the activity of these methyltransferase family members.

DISCUSSION

Mitochondrial RNA Methyltransferase Family Members—Ribosomal RNAs invariably contain post-transcriptional modifications that alter the structure of the RNA, commonly in sites buried within the RNA in relatively protein-free regions important for ribosomal function (5). In bacteria, rRNA methylation reactions are catalyzed by dedicated site-specific modifying enzymes, whereas nuclear/cytoplasmic ribosomes of higher eukaryotes typically contain machinery that employs guide RNAs to direct these events. In keeping with their prokaryotic ancestry, yeast mitochondria employ individual enzymes for rRNA methylation. In yeast, 2'-O-ribose modification by

Pet56p generates Gm²²⁷⁰, whereas Mrm2p generates Um²⁷⁹¹ (17, 18). Although these modifications are separated by over 500 nucleotides in the primary sequence, they both fold into the peptidyltransferase center of the mitochondrial ribosome (38).

In this study, we have confirmed the mitochondrial localization of three mammalian members of the methyltransferase family. Two of these, MRM1 and RNMTL1, closely resemble yeast Pet56p in their content of 2'-O-ribose binding domains and SPOUT family domains. The third, FtsJ2 or MRM2, is more closely related to yeast MRM2 and *E. coli* RLME uridyl-2'-O-methyltransferases. These sequence relationships suggest that mammalian MRM2 is most likely to be involved in the single known uridyl 2'-O-ribose methylation at U¹³⁶⁹ in human 16 S rRNA. MRM1 and RNMTL1, then, may be involved in 2'-O-ribose modifications at G¹¹⁴⁵ and G¹³⁷⁰ of human 16 S rRNA. Our primer extension results (Fig. 10) suggest that RNMTL1 is likely to be involved in the modification of G¹³⁷⁰, although, as noted above, the adjacent modification at U¹³⁶⁹ complicates this analysis. It remains to be determined whether methylation requires additional factors or a partially assembled ribosome as substrate. Here, we have primarily focused on the implications of our finding that all three putative mammalian mitochondrial methyltransferases are localized near mtDNA nucleoids.

Nucleoid and Ribosome Association of RNA Methyltransferase Family Members—We initially identified RNMTL1 as a nucleoid-associated protein using proteomic analysis of formaldehyde-cross-linked proteins (21). In this paper, we show that significant fractions of RNMTL1 and MRM1 co-sediment with nucleoids (Fig. 4) and remain associated with nucleoids through isopycnic sedimentation in non-ionic density gradients (Fig. 5). Our current cell fractionation experiments did not use cross-linking agents to stabilize large complexes. Under these conditions, more loosely associated proteins and complexes are readily dissociated from the large nucleoid. In fact, we routinely see a substantial fraction of TFAM released from nucleoids during the initial sedimentation (39). Our failure to identify MRM1 in our earlier study of cross-linked nucleoids may indicate that it was not effectively cross-linked to DNA complexes. Alternatively, the quantity of MRM1 protein in these specimens may have been below the detection limit of the Q-STAR mass spectrometer used at that time. We have routinely observed both MRM1 and RNMTL1 but not MRM2 in more recent biochemical preparations of nucleoids using more sensitive Orbitrap mass spectrometric analysis (data not shown). Here we report that all three rRNA methyltransferase family members considered in this study were found to be selectively localized at or near nucleoids using laser confocal scanning microscopy (Fig. 2). Stable nucleoid association may require that the protein remain associated with nascent mtRNA resident in transcription elongation complexes. Although the rRNAs may remain in the vicinity of nucleoids as ribosome assembly continues, these later assembly intermediates may readily dissociate from nucleoids upon mitochondrial lysis and sedimentation. He *et al.* (40) have also found ribosomes closely associated with nucleoids in iodixanol gradients. However, because both nucleoids and ribosomes are protein-nucleic acid complexes, their densities are sufficiently close in these gradients that we prefer to use sedimentation for the initial separation followed

by an iodixanol gradient for more effective separation. This has permitted us to document separate pools of RNMTL1 associated with nucleoids and with ribosomes. We have found that down-regulation of RNMTL1 using siRNA leads to a significant inhibition of mitochondrial translation (Fig. 9). RNMTL1 exhibits persistent binding to the large ribosomal subunit during glycerol gradient sedimentation in the presence of EDTA, during sucrose gradient sedimentation in 20 mM MgCl₂, and in non-ionic density gradients, although association with the ribosome is reduced when sedimentation is performed in 20 mM MgCl₂. This behavior contrasts with that of MRML1, which shows minimal association with ribosomes.

A number of recent studies have revealed that numerous proteins involved in mtRNA processing and degradation are enriched in punctate foci near nucleoids. These structures have been referred to as mitochondrial RNA granules (41, 42) or degradosome foci (D-foci (43)), depending on the proteins investigated in a particular study. Clearly, it is a high priority to determine the spatial relationships among complexes containing potential rRNA methyltransferases, RNA granule proteins, and SUV3L1/PNPase degradosome components to better understand processing events. This will require superresolution imaging methods (44–47) of the sort used recently to study the structure of the mtDNA nucleoid core (31, 48). These methods have revealed that mtDNA nucleoids are commonly oblate spheroids with axial dimensions of about 100–130 nm or sometimes larger, irregular complexes nestled between adjacent folds of the mitochondrial cristae (49).

These recent imaging studies, along with our results (Figs. 2 and 3) support the general hypothesis that nascent mtRNA is processed in dynamic foci in the vicinity of nucleoids. We suggest that rRNA modification and ribosome assembly are among the key processing steps centered around nucleoids. A large number of publications have established that ribosome assembly begins while transcription is proceeding both in bacteria (16, 50) and in the eukaryotic nucleolus (51, 52). The concept that assembly of mitochondrial ribosomes is initiated near nucleoids may reflect a dynamic coupling between transcription, RNA methylation, and ribosome assembly. This would help to explain two other recent findings. First, Surovtseva and Shadel (53) reported that mtRNA polymerase has a transcription-independent role in ribosome assembly, dependent to some degree on the interaction of mtRNA polymerase with the methyltransferase TFB1M. Second, Larsson's group (54) has shown that MTERF3 is both a negative regulator of mitochondrial transcription and a factor involved in mitochondrial ribosome assembly (55). MTERF3 and mtRNA polymerase were both identified as interacting with RNMTL1, possibly mediated by RNA structures (Table 1). Elegant experiments have shown that the rate of transcription by nuclear RNA polymerase I is coupled to events in rRNA modification and ribosome assembly (56). MTERF3 and the complex of MTERF4-NSUN4 may operate in a similar manner in mitochondria (19). Our identification of proteins associated with RNMTL1 offers significant support for this model. In addition to mtRNA polymerase and MTERF3, we found RNA chaperones LRPPRC (57–59), GRSF1 (41, 42), p32/gC1qR (60), and PTCD3 (61); protein chaperones HSP60 and HSP75; and the probable RNA helicase DDX28

associated with RNMTL1 complexes (Table 1). Numerous RNA helicases have been shown to function in assembly of eukaryotic ribosomes (52). It is interesting to note that another helicase we previously found to be highly represented in nucleoids, DHX30, was not found associated with RNMTL1. The identification of these interacting partners opens the door to experiments to further define mechanisms that regulate transcription, rRNA modification, and ribosome assembly in mitochondria.

Acknowledgments—We thank Dr. Linda Spremulli for a gift of antibodies directed against MRPL13, Dr. Miguel Garcia-Diaz for other reagents, and Antonius Koller of the Stony Brook University proteomics service for assistance.

REFERENCES

- Sharma, M. R., Koc, E. C., Datta, P. P., Booth, T. M., Spremulli, L. L., and Agrawal, R. K. (2003) Structure of the mammalian mitochondrial ribosome reveals an expanded functional role for its component proteins. *Cell* **115**, 97–108
- Koc, E. C., Haque, M. E., and Spremulli, L. L. (2010) Current views of the structure of the mammalian mitochondrial ribosome. *Isr. J. Chem.* **50**, 45–59
- Christian, B. E., and Spremulli, L. L. (2012) Mechanism of protein biosynthesis in mammalian mitochondria. *Biochim. Biophys. Acta* **1819**, 1035–1054
- Leach, K. L., Swaney, S. M., Colca, J. R., McDonald, W. G., Blinn, J. R., Thomasco, L. M., Gadwood, R. C., Shinabarger, D., Xiong, L., and Mankin, A. S. (2007) The site of action of oxazolidinone antibiotics in living bacteria and in human mitochondria. *Mol. Cell* **26**, 393–402
- Decatur, W. A., and Fournier, M. J. (2002) rRNA modifications and ribosome function. *Trends Biochem. Sci.* **27**, 344–351
- Baer, R. J., and Dubin, D. T. (1981) Methylated regions of hamster mitochondrial ribosomal RNA. Structural and functional correlates. *Nucleic Acids Res.* **9**, 323–337
- Dubin, D. T., and Taylor, R. H. (1978) Modification of mitochondrial ribosomal RNA from hamster cells. The presence of GmG and late-methylated UmGmU in the large subunit (17S) RNA. *J. Mol. Biol.* **121**, 523–540
- Rorbach, J., and Minczuk, M. (2012) The post-transcriptional life of mammalian mitochondrial RNA. *Biochem. J.* **444**, 357–373
- Connolly, K., Rife, J. P., and Culver, G. (2008) Mechanistic insight into the ribosome biogenesis functions of the ancient protein KsgA. *Mol. Microbiol.* **70**, 1062–1075
- Mangat, C. S., and Brown, E. D. (2008) Ribosome biogenesis. The KsgA protein throws a methyl-mediated switch in ribosome assembly. *Mol. Microbiol.* **70**, 1051–1053
- Seidel-Rogol, B. L., McCulloch, V., and Shadel, G. S. (2003) Human mitochondrial transcription factor B1 methylates ribosomal RNA at a conserved stem-loop. *Nat. Genet.* **33**, 23–24
- Metodiey, M. D., Lesko, N., Park, C. B., Cámara, Y., Shi, Y., Wibom, R., Hultenby, K., Gustafsson, C. M., and Larsson, N.-G. (2009) Methylation of 12S rRNA is necessary for *in vivo* stability of the small subunit of the mammalian mitochondrial ribosome. *Cell Metab.* **9**, 386–397
- Raimundo, N., Song, L., Shutt, T. E., McKay, S. E., Cotney, J., Guan, M.-X., Gilliland, T. C., Hohuan, D., Santos-Sacchi, J., and Shadel, G. S. (2012) Mitochondrial stress engages E2F1 apoptotic signaling to cause deafness. *Cell* **148**, 716–726
- Dennerlein, S., Rozanska, A., Wydro, M., Chrzanowska-Lightowlers, Z. M., and Lightowlers, R. N. (2010) Human ERAL1 is a mitochondrial RNA chaperone involved in the assembly of the 28S small mitochondrial ribosomal subunit. *Biochem. J.* **430**, 551–558
- Uchiyama, T., Ohgaki, K., Yagi, M., Aoki, Y., Sakai, A., Matsumoto, S., and Kang, D. (2010) ERAL1 is associated with mitochondrial ribosome and elimination of ERAL1 leads to mitochondrial dysfunction and growth re-

- tardation. *Nucleic Acids Res.* **38**, 5554–5568
16. Kaczanowska, M., and Rydén-Aulin, M. (2007) Ribosome biogenesis and the translation process in *Escherichia coli*. *Microbiol. Mol. Biol. Rev.* **71**, 477–494
 17. Sirum-Connolly, K., and Mason, T. (1993) Functional requirement of a site-specific ribose methylation in ribosomal RNA. *Science* **262**, 1886–1889
 18. Pintard, L., Bujnicki, J. M., Lapeyre, B., and Bonnerot, C. (2002) MRM2 encodes a novel yeast mitochondrial 21S rRNA methyltransferase. *EMBO J.* **21**, 1139–1147
 19. Cámara, Y., Asin-Cayuela, J., Park, C. B., Metodieff, M. D., Shi, Y., Ruzzenente, B., Kukat, C., Habermann, B., Wibom, R., Hultenby, K., Franz, T., Erdjument-Bromage, H., Tempst, P., Hallberg, B. M., Gustafsson, C. M., and Larsson, N.-G. (2011) MTERF4 regulates translation by targeting the methyltransferase NSUN4 to the mammalian mitochondrial ribosome. *Cell Metab.* **13**, 527–539
 20. Lafontaine, D. L., Preiss, T., and Tollervey, D. (1998) Yeast 18S rRNA dimethylase Dim1p. A quality control mechanism in ribosome synthesis? *Mol. Cell Biol.* **18**, 2360–2370
 21. Bogenhagen, D. F., Rousseau, D., and Burke, S. (2008) The layered structure of human mitochondrial DNA nucleoids. *J. Biol. Chem.* **283**, 3665–3675
 22. Pagliarini, D. J., Calvo, S. E., Chang, B., Sheth, S. A., Vafai, S. B., Ong, S.-E., Walford, G. A., Sugiana, C., Boneh, A., Chen, W. K., Hill, D. E., Vidal, M., Evans, J. G., Thorburn, D. R., Carr, S. A., and Mootha, V. K. (2008) A mitochondrial protein compendium elucidates complex I disease biology. *Cell* **134**, 112–123
 23. Ching, Y.-P., Zhou, H.-J., Yuan, J.-G., Qiang, B.-Q., Kung, H.-f., and Jin, D.-Y. (2002) Identification and characterization of FTSJ2, a novel human nuclear protein homologous to bacterial ribosomal RNA methyltransferase. *Genomics* **79**, 2–6
 24. Brown, T. A., Fetter, R. D., Tkachuk, A. N., and Clayton, D. A. (2010) Approaches toward super-resolution fluorescence imaging of mitochondrial proteins using PALM. *Methods* **51**, 458–463
 25. McKinney, S. A., Murphy, C. S., Hazelwood, K. L., Davidson, M. W., and Looger, L. L. (2009) A bright and photostable photoconvertible fluorescent protein. *Nat. Methods* **6**, 131–133
 26. Trounce, I. A., Kim, Y. L., Jun, A. S., and Wallace, D. C. (1996) Assessment of mitochondrial oxidative phosphorylation in patient muscle biopsies, lymphoblasts, and transmittochondrial cell lines. *Methods Enzymol.* **264**, 484–509
 27. Kellems, R. E., Allison, V. F., and Butow, R. A. (1975) Cytoplasmic type 80S ribosomes associated with yeast mitochondria. IV. Attachment of ribosomes to the outer membrane of isolated mitochondria. *J. Cell Biol.* **65**, 1–14
 28. Chomyn, A. (1996) *In vivo* labeling and analysis of human mitochondrial translation products. *Methods in Enzymology* **264**, 197–211
 29. Luongo, C. L., Contreras, C. M., Farsetta, D. L., and Nibert, M. L. (1998) Binding site for *S*-adenosyl-L-methionine in a central region of mammalian reovirus lambda2 protein. Evidence for activities in mRNA cap methylation. *J. Biol. Chem.* **273**, 23773–23780
 30. Holzmann, J., Frank, P., Löffler, E., Bennett, K. L., Gerner, C., and Rossmanith, W. (2008) RNase P without RNA. Identification and functional reconstitution of the human mitochondrial tRNA processing enzyme. *Cell* **135**, 462–474
 31. Brown, T. A., Tkachuk, A. N., Shtengel, G., Kopeck, B. G., Bogenhagen, D. F., Hess, H. F., and Clayton, D. A. (2011) Superresolution fluorescence imaging of mitochondrial nucleoids reveals their spatial range, limits, and membrane interaction. *Mol. Cell Biol.* **31**, 4994–5010
 32. Bogenhagen, D. F., Wang, Y., Shen, E. L., and Kobayashi, R. (2003) Protein components of mitochondrial DNA nucleoids in higher eukaryotes. *Mol. Cell Proteomics* **2**, 1205–1216
 33. Koc, E. C., Cimen, H., Kumcuoglu, B., Abu, N., Akpınar, G., Haque, M. E., Spremulli, L. L., and Koc, H. (2013) Identification and characterization of CHCHD1, AURKAIP1, and CRIF1 as new members of the mammalian mitochondrial ribosome. *Front. Physiol.* **4**, 183
 34. Maden, B. E., Corbett, M. E., Heeney, P. A., Pugh, K., and Ajuh, P. M. (1995) Classical and novel approaches to the detection and localization of the numerous modified nucleotides in eukaryotic ribosomal RNA. *Biochimie* **77**, 22–29
 35. Tkaczuk, K. L., Dunin-Horkawicz, S., Purta, E., and Bujnicki, J. M. (2007) Structural and evolutionary bioinformatics of the SPOUT superfamily of methyltransferases. *BMC Bioinformatics* **8**, 73
 36. Yakubovskaya, E., Guja, K. E., Mejia, E., Castano, S., Hambardjjeva, E., Choi, W. S., and Garcia-Diaz, M. (2012) Structure of the essential MTERF4:NSUN4 protein complex reveals how an MTERF protein collaborates to facilitate rRNA modification. *Structure* **20**, 1940–1947
 37. Spähr, H., Habermann, B., Gustafsson, C. M., Larsson, N.-G., and Hallberg, B. M. (2012) Structure of the human MTERF4-NSUN4 protein complex that regulates mitochondrial ribosome biogenesis. *Proc. Natl. Acad. Sci. U.S.A.* **109**, 15253–15258
 38. Mears, J. A., Sharma, M. R., Gutell, R. R., McCook, A. S., Richardson, P. E., Caulfield, T. R., Agrawal, R. K., and Harvey, S. C. (2006) A structural model for the large subunit of the mammalian mitochondrial ribosome. *J. Mol. Biol.* **358**, 193–212
 39. Wang, Y., and Bogenhagen, D. F. (2006) Human mitochondrial DNA nucleoids are linked to protein folding machinery and metabolic enzymes at the mitochondrial inner membrane. *J. Biol. Chem.* **281**, 25791–25802
 40. He, J., Cooper, H. M., Reyes, A., Di Re, M., Sembongi, H., Litwin, T. R., Gao, J., Neuman, K. C., Fearnley, I. M., Spinazzola, A., Walker, J. E., and Holt, I. J. (2012) Mitochondrial nucleoid interacting proteins support mitochondrial protein synthesis. *Nucleic Acids Res.* **40**, 6109–6121
 41. Antonicka, H., Sasarman, F., Nishimura, T., Paupe, V., and Shoubridge, E. A. (2013) The mitochondrial RNA-binding protein GRSF1 localizes to RNA granules and is required for posttranscriptional mitochondrial gene expression. *Cell Metabolism* **17**, 386–398
 42. Jourdain, A. A., Koppen, M., Wydro, M., Rodley, C. D., Lightowlers, R. N., Chrzanowska-Lightowlers, Z. M., and Martinou, J.-C. (2013) GRSF1 regulates RNA processing in mitochondrial RNA granules. *Cell Metab.* **17**, 399–410
 43. Borowski, L. S., Dziembowski, A., Hejnowicz, M. S., Stepien, P. P., and Szczesny, R. J. (2013) Human mitochondrial RNA decay mediated by PNPase-hSuv3 complex takes place in distinct foci. *Nucleic Acids Res.* **41**, 1223–1240
 44. Hell, S. W. (2009) Microscopy and its focal switch. *Nat. Methods* **6**, 24–32
 45. Huang, B., Bates, M., and Zhuang, X. (2009) Super-resolution fluorescence microscopy. *Annu. Rev. Biochem.* **78**, 993–1016
 46. Fischer, R. S., Wu, Y., Kanchanawong, P., Shroff, H., and Waterman, C. M. (2011) Microscopy in 3D. A biologist's toolbox. *Trends Cell Biol.* **21**, 682–691
 47. Schermelleh, L., Heintzmann, R., and Leonhardt, H. (2010) A guide to super-resolution fluorescence microscopy. *J. Cell Biol.* **190**, 165–175
 48. Kukat, C., Wurm, C. A., Spähr, H., Falkenberg, M., Larsson, N.-G., and Jakobs, S. (2011) Super-resolution microscopy reveals that mammalian mitochondrial nucleoids have a uniform size and frequently contain a single copy of mtDNA. *Proc. Natl. Acad. Sci.* **108**, 13534–13539
 49. Kopeck, B. G., Shtengel, G., Xu, C. S., Clayton, D. A., and Hess, H. F. (2012) Correlative 3D superresolution fluorescence and electron microscopy reveal the relationship of mitochondrial nucleoids to membranes. *Proc. Natl. Acad. Sci. U.S.A.* **109**, 6136–6141
 50. Shajani, Z., Sykes, M. T., and Williamson, J. R. (2011) Assembly of bacterial ribosomes. *Annu. Rev. Biochem.* **80**, 501–526
 51. Fatica, A., and Tollervey, D. (2002) Making ribosomes. *Curr. Opin. Cell Biol.* **14**, 313–318
 52. Kressler, D., Hurt, E., and Bassler, J. (2010) Driving ribosome assembly. *Biochim. Biophys. Acta* **1803**, 673–683
 53. Surovtseva, Y. V., and Shadel, G. S. (2013) Transcription-independent role for human mitochondrial RNA polymerase in mitochondrial ribosome biogenesis. *Nucleic Acids Res.* **41**, 2479–2488
 54. Park, C. B., Asin-Cayuela, J., Cámara, Y., Shi, Y., Pellegrini, M., Gaspari, M., Wibom, R., Hultenby, K., Erdjument-Bromage, H., Tempst, P., Falkenberg, M., Gustafsson, C. M., and Larsson, N.-G. (2007) MTERF3 is a negative regulator of mammalian mtDNA transcription. *Cell* **130**, 273–285
 55. Wredenberg, A., Lagouge, M., Bratic, A., Metodieff, M. D., Spähr, H., Mourier, A., Freyer, C., Ruzzenente, B., Tain, L., Grönke, S., Baggio, F., Kukat, C., Kremmer, E., Wibom, R., Polosa, P. L., Habermann, B., Par-

- tridge, L., Park, C. B., and Larsson, N.-G. (2013) MTERF3 regulates mitochondrial ribosome biogenesis in invertebrates and mammals. *PLoS Genet.* **9**, e1003178
56. Schneider, D. A., Michel, A., Sikes, M. L., Vu, L., Dodd, J. A., Salgia, S., Osheim, Y. N., Beyer, A. L., and Nomura, M. (2007) Transcription elongation by RNA polymerase I is linked to efficient rRNA processing and ribosome assembly. *Mol. Cell* **26**, 217–229
57. Gohil, V. M., Nilsson, R., Belcher-Timme, C. A., Luo, B., Root, D. E., and Mootha, V. K. (2010) Mitochondrial and nuclear genomic responses to loss of LRPPRC expression. *J. Biol. Chem.* **285**, 13742–13747
58. Ruzzenente, B., Metodiev, M. D., Wredenberg, A., Bratic, A., Park, C. B., Cámara, Y., Milenkovic, D., Zickermann, V., Wibom, R., Hultenby, K., Erdjument-Bromage, H., Tempst, P., Brandt, U., Stewart, J. B., Gustafsson, C. M., and Larsson, N.-G. (2012) LRPPRC is necessary for polyadenylation and coordination of translation of mitochondrial mRNAs. *EMBO J.* **31**, 443–456
59. Antonicka, H., Ostergaard, E., Sasarman, F., Weraarpachai, W., Wibrand, F., Pedersen, A. M., Rodenburg, R. J., van der Knaap, M. S., Smeitink, J. A., Chrzanowska-Lightowlers, Z. M., and Shoubridge, E. A. (2010) Mutations in C12orf65 in patients with encephalomyopathy and a mitochondrial translation defect. *Am. J. Hum. Genet.* **87**, 115–122
60. Yagi, M., Uchiumi, T., Takazaki, S., Okuno, B., Nomura, M., Yoshida, S., Kanki, T., and Kang, D. (2012) p32/gC1qR is indispensable for fetal development and mitochondrial translation. Importance of its RNA-binding ability. *Nucleic Acids Res.* **40**, 9717–9737
61. Davies, S. M., Rackham, O., Shearwood, A.-M., Hamilton, K. L., Narsai, R., Whelan, J., and Filipovska, A. (2009) Pentatricopeptide repeat domain protein 3 associates with the mitochondrial small ribosomal subunit and regulates translation. *FEBS Lett.* **583**, 1853–1858
62. Caldas, T., Binet, E., Bouloc, P., Costa, A., Desgres, J., and Richarme, G. (2000) The FtsJ/RrmJ heat shock protein of *Escherichia coli* is a 23 S ribosomal RNA methyltransferase. *J. Biol. Chem.* **275**, 16414–16419